Trauma Case Reports 49 (2024) 100978

Contents lists available at ScienceDirect

Trauma Case Reports

journal homepage: www.elsevier.com/locate/tcr

Case Report

A 3D-printed load sharing implant achieved union of a 9-cm femoral segmental bone defect within three months using a hybrid Masquelet induction membrane technique. A case-report

Athanasios F. Foukas [a], Argyris C. Hadjimichael [b,*], Christophoros Nicolaou [c], Olga D. Savvidou [d], Panayiotis J. Papagelopoulos [d]

[a] Third Department of Orthopaedic Surgery, "KAT" General Hospital of Athens, 2, Nikis Street, 14561 Kifissia, Greece
[b] Orthopaedic Department, Saint Mary's and John's Polyclinic, 2, Karditsis Street, 2045 Nicosia, Cyprus
[c] Radiology Department, Aretaeio Private Hospital, 55-57, Andrea Avraamides, Strovolos 2024, Nicosia, Cyprus
[d] First Department of Orthopaedic Surgery, National and Kapodistrian University of Athens, Faculty of Medicine, Attikon University Hospital, 1 Rimini Street, Chaidari, 12462 Athens, Greece

ARTICLE INFO

Keywords:
Bone defect
Masquelet
Customized
3D-printed
Union

ABSTRACT

Case: A 30-year-old male was admitted in our hospital having an open left distal femoral fracture with 9-cm segmental bone defect and a closed proximal left tibial fracture. He was treated successfully using a Hybrid (Titanium Cage and Bone Graft) Masquelet Induction Membrane Technique (MIMT). His femoral fracture united 3-months post - operatively. The left tibia was treated initially with two locking plates. Following infection, a 3-cm tibial bone gap was treated with external fixation and conventional MIMT. The tibial fracture united 12-months post- operatively. *Conclusion:* The Hybrid MIMT achieved a successful healing outcome in this challenging case.

Introduction

The technology of additive manufacturing allows the production of precise personalized orthopaedic products to meet patient needs with difficult structural bone problems. Standard implants do not always provide reliable solutions in cases with large bone defects. 3D- printed custom-made implants however, already have a successful clinical record to treat challenging bone losses [1].

The use of 3D-printed guides and models in orthopaedics is associated with significantly shorter operating times and cost-effective treatments [2].

Cost savings could be maximized in case custom-made implants are used to deal with massive bone losses, minimizing even further operative times, reducing the number of operative procedures, as well as speeding up rehabilitation.

Several studies in the literature report, that patient-specific 3D-printed titanium cages loaded with bone graft, are advantageous when inserted into a foreign body-induced membrane in cases of massive juxta-articular distal femoral bone loss [3,4].

Case presentation

A 30-year-old male patient was transferred to our hospital's emergency department. He had been involved in a motorcycle accident

* Corresponding author.
E-mail addresses: afoukas1@otenet.gr (A.F. Foukas), ortho.argiris@gmail.com (A.C. Hadjimichael).

https://doi.org/10.1016/j.tcr.2024.100978
Accepted 15 January 2024
Available online 19 January 2024

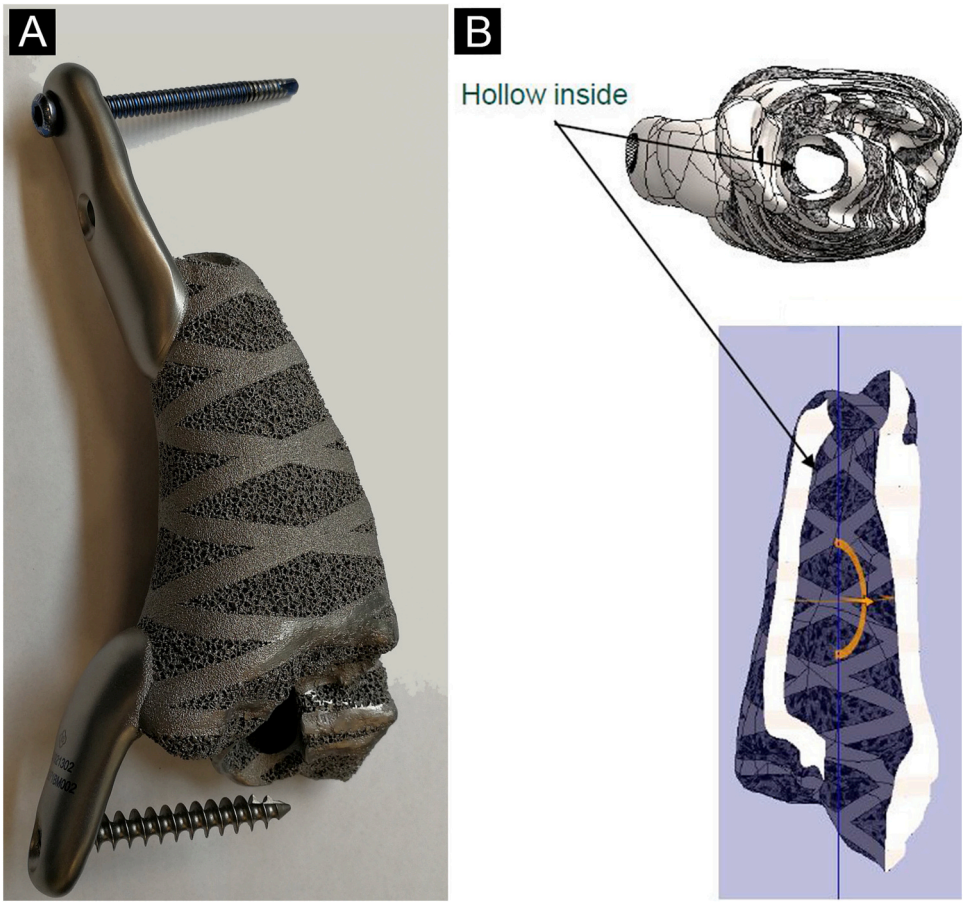

Fig. 1. A. The 3D-printed load sharing implant to cover a 9-cm femoral bone defect.
The 3D-printed custom-made load cage was manufactured by Implantcast® GmbH as a load sharing bone scaffold and a bone graft container. The new manufacturing method of EBM® (Electron Beam Melting) is a process invested and used by Implantcast GmbH which offers a rapid, flexible and cost-effective implant directly from patients' 3D electronic data. The 3D-printed cage is an EPORE® (EPORE® isa registered trademark of Implantcast GmbH) highly porous structure made of titanium alloy (Ti6AlV4). Titanium alloy is an excellent material for use as a porous ingrowth structure as it is biologically inert, ductile, corrosion resistant and has a high fatigue strength. Implantcast GmbH EPORE® design is characterized by high porosity and a low modulus of elasticity, supporting biological ingrowth. The EPORE® structure is specified by rods of 330–390 μm thickness which are arrayed in a way that mimics cancellous bone structures.
B. The micro-architecture of the 3D-printed implant.
The image shows the EPORE® 3D-printed implant (solid material in double helix form) from above and inside, appropriate for bone ingrowth and fluid exchange. EPORE® is designed to match natural cancellous bone structure that improves the osseous- integration process of the new prosthesis.

driving at 80 km/h. He had been taken initially into a different hospital, where a right trans-femoral amputation had been performed as a life- saving procedure [5]. The patient arrived the following day into our A & E department intubated due to GCS of 8 upon his arrival at the referring hospital.

He had critical limb ischemia due to a left floating knee. His left leg had been immobilized in a plaster of Paris back and U-slab. The floating knee was associated with an open left distal femoral trans-condylar fracture and a closed transverse left proximal tibial and fibular fracture with extensive skin abrasions and contusions. He was taken to theatre, where a cross-knee external fixator was applied on the left femur and left tibia. Manual indirect reduction of the fractures were achieved. An angiogram performed following reduction, revealed a restored blood supply to his left lower limb. The femoral wound edges as well as all non-viable bone and muscle were debrided. 80 % rupture of quadricep's tendon (3 cm proximal to the patella) was diagnosed. The rupture was repaired primarily. His femoral wound was left open and covered with povidone iodine-impregnated dressings by the plastic surgeons. He had a CT scan on his head and neck following a neurosurgical examination in theatre. The CT scan revealed diffuse cerebral edema. He was then transferred to our Intensive Care Unit (ICU). The Masquelet technique was chosen to reconstruct his type III,9-cm long segmental bone loss a week later during a second look operation [6,7]. The femoral condyles and femoral shaft were directly reduced and fixed with a laterally based AxSOS (Stryker) condylar locking plate. A 9-cm block of a gentamycin- impregnated PMMA cement spacer was placed in the bone gap extending over the fracture ends as well as over the stainless-steel plate to induce an angiogenic and osteoinductive membrane. The surgical wound was closed, whilst the initial wound was left open and covered with povidone iodine-impregnated

Fig. 2. X-ray of the left femur three weeks after the placement of the customized 3D- printed implant.
X-ray of the distal femur reveals the 3D-printed implant and the graft which were inserted within the induced PMMA osteogenic membrane.

dressings. The cross-knee external fixator was left in place, as reduction of the proximal tibia was satisfactory in terms of apposition and alignment. A decision was made to proceed with a 3D-printed load-sharing scaffold to not only contain the autologous bone graft in the femur during the next stage, but to supplement biomechanically the stainless-steel locking plate and proceed with early aggressive knee mobilization and immediate weight bearing as well. A detailed O-MAR CT scan was performed (1 mm slices) of the left femur with the plate and the cement spacer in situ including the left tibia, left ankle and foot. Eight weeks later plain femoral x-rays revealed enhanced osteogenic activity of the induced membrane around the cement spacer. This rapid rate of ossification around the cement spacer was surprising to us. We expected the development of an osteogenic membrane. However, the enhanced spontaneous ossification of the induction membrane in this patient was attributed to the dual effects of traumatic brain injury as well as the

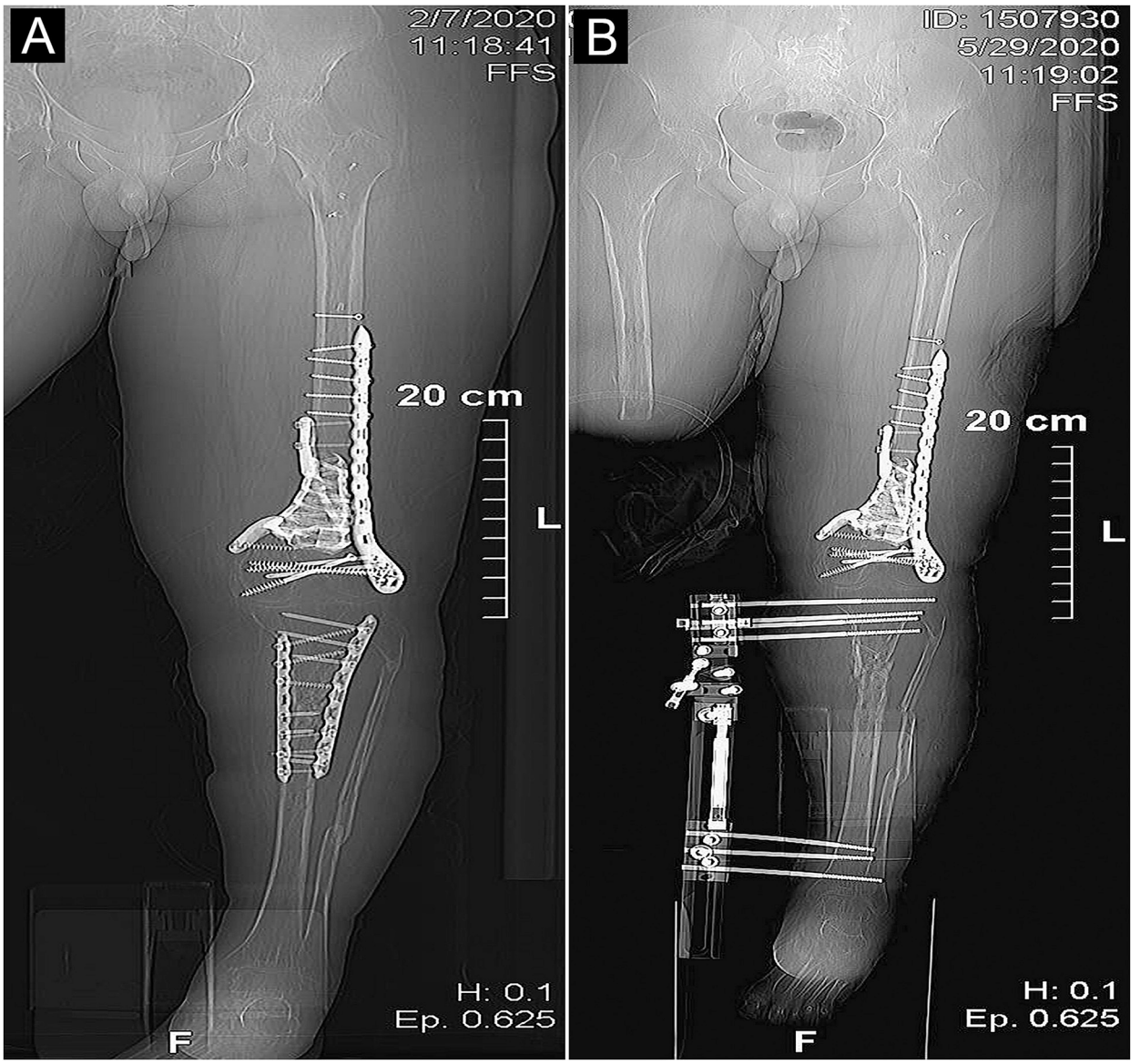

Fig. 3. A. Axonometric view of the left lower limb 3-months after implantation of the femur and double ORIF of left tibia.
The x-ray shows appropriate alignment and bone healing of the femur using the personalized 3D-printed implants well as the placement of one anterior lateral and one medial locking plates at 90° to each other on the left tibial fracture. Date of examination: 7, February 2020 as shown in the fig.
B. Axonometric view of the left lower limb performed 3-months after tibial internal fixation. Both plates were removed due to infection.
Following infection, the tibial metalwork was removed. Infected bone and soft tissues were debrided. Polymethyl methacrylate gentamycin plus vancomycin impregnated cement was applied in the residual 3-cm fracture gap. A Unilateral Limb Reconstruction External Fixator System was applied to stabilize the fracture and a fibular osteotomy was performed. Date of examination: 29, May 2020 as shown in the figure.

induction membrane technique [8,9]. During the next operative procedure, a longitudinal incision was made on the partially ossified induced membrane and the bone cement was removed. We then used the Reamer Irrigator.

Aspirator (RIA) System (Depuy Synthes, Oberdorf, Switzerland), to harvest autologous bone graft from the ipsilateral proximal femur. To ensure adequate quantities of bone graft we ordered cancellous allograft as well, to fill in the cavities of the 3D-printed custom-made load cage (manufactured by Implantcast® GmbH as a load-sharing bone scaffold and a bone graft container, as shown in Fig. 1A and B) and manage the osseous gap in the ipsilateral tibia. The surgeon (AFF) was involved in the process of designing the implant, so that planned surgical approach, screw trajectories and plate constructs, were all incorporated into the design. The graft volume required was about 100 cc. The harvested autograft was augmented with allograft cancellous chips during surgery. The graft was digitally impacted into the cavity of the implant (40 cc volume), as well as on the surface of the implant and the host bone-implant

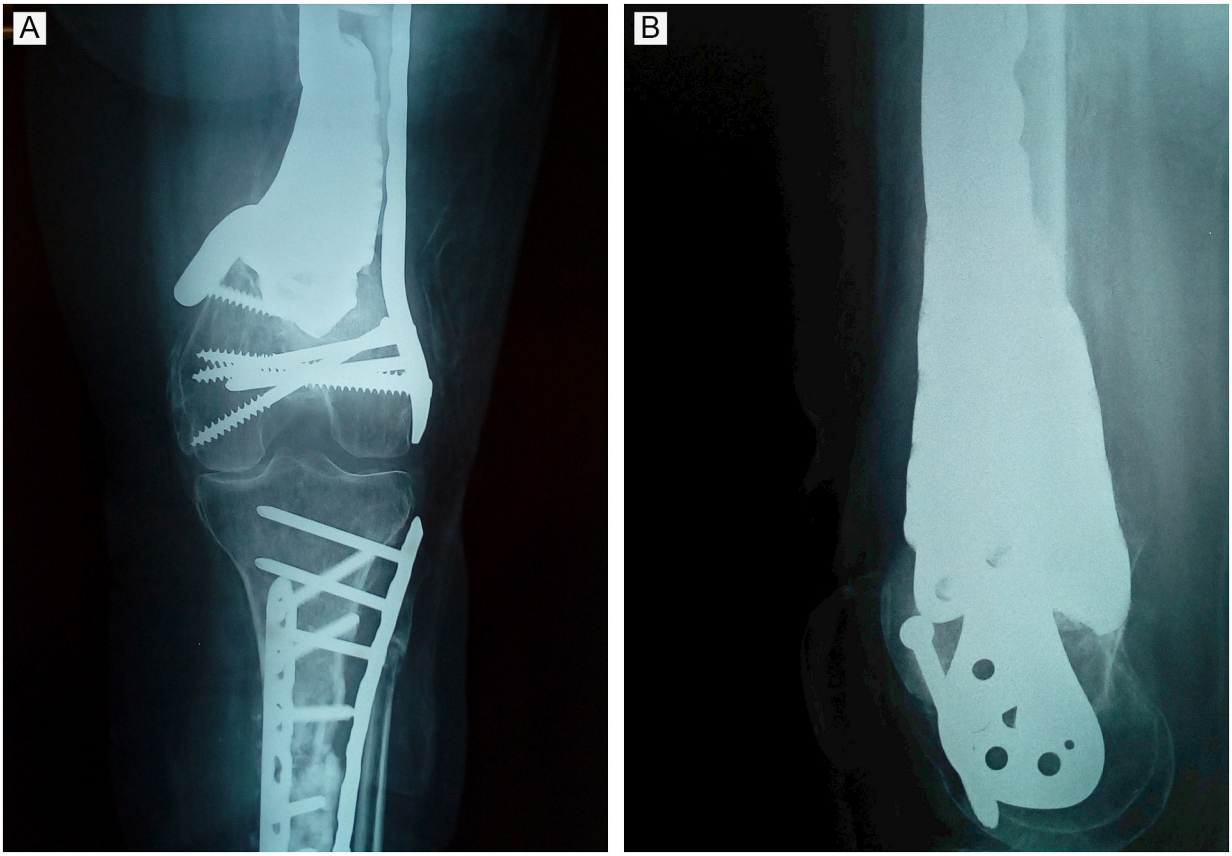

Fig. 4. A and B. AP and lateral radiographs showing full osseointegration of the 3D printed implant in the femur 3-months postoperatively. Osseointegration in bone - EPORE material bone interface junctions are scored 4/4 (2 points on AP and 2 points on lateral film). Based on the on-growth grading system a stage 4 osseointegration, reveals the highest grade of union.

junctions (another 40 cc). The device was then fitted carefully within the PMMA membrane envelope defined by the fracture ends and the plate, using arthroscopic bone burrs when necessary. Using an image intensifier, two small incisions were performed to fix the implant's side plates on the left femur with cortical and cancellous screws, as seen in Fig. 2. Before the final fixation of the implant's side plates, the AXSOS femoral plate was re-tensioned using the AO articulated tension device. All tissue specimens sent for microbiology cultures before and after insertion of the custom-made implant were did not grow any microorganisms.

Surgical management of left tibia fracture included the application of one anterior lateral and one medial locking plate at 90° to each other (as shown in Fig. 3A), along with the application of cancellous bone autograft and allograft (20 cc) to deal with a 2-cm medially based cortical tibia defect. That was performed by another surgical team within the same operative session.

Our patient developed septicemia in ICU, due to an abscess of his gallbladder that was treated with an open cholecystectomy. He remained in ICU for another four weeks. Eight weeks following his definitive fixation of femur and tibia, his wounds looked healthy. X-rays of his left femur and left tibia looked satisfactory. After the above knee prosthesis was fitted on his amputated lower limb our patient was able to weight bear on his left lower limb using a Zimmer frame without any pain on his left femur.

A CT scan of his left femur revealed full osseointegration of his 3D- printed cage into his left femur. The CT scan and x-rays of his distal femur revealed bone ingrowth into the 3D-printed implant within 3 months and progress of union on his left proximal tibial fracture, as shown in Fig. 3B. Three radiology consultants independently reviewed the plain radiographs, with disagreements resolved by consensus. Osseointegration was defined as the presence of extraosseous bone growth overlying the EPORE material bone interface without a radiolucent line between the new bone growth and the EPORE. According to the study by Davies et al. [10], the osteointegration to HA-coated collars of cemented massive endoprostheses was classified by two methods:

1. Zone score 11 – osseointegration scored 0 to 4, according to the number of bone-collar junctions where osseointegration was seen (up to 2 on AP and 2 on lateral films).
2. On growth grading 22 – osseointegration graded based in AP and lateral plain x-rays as following: Grade 1: No osseointegration or bone growth. b) Grade 2: Bone growth around collar with gap between new bone and collar. c) Grade 3: Osseointegration in 1 or 2 zones. d) Grade 4: Osseointegration in 3 or 4 zones [10,11]. Both grade 1 and 2 represent failure to osteo-integrate to the HA-coated

Fig. 5. A. CT scan image of the left tibia 12-months post- operatively, demonstrating sufficient union of the tibial fracture.
The anteroposterior CT scan image demonstrates the radiological union of the tibial fracture 12- months after the insertion of bone graft within the Masquelet tibial induction membrane which was correlated with excellent clinical outcomes and no signs of infection.
B. CT scan image of the femur 12-months after its implantation.
CT scan images reveal stable internal fixation as well as the osseo-integration progress of the customized 3D-printed implant in the femur.

collar. Serial postoperative radiographs were reviewed to identify at what time osseointegration first occurred. Fig. 4A and B depicts the 3-month AP and lateral radiograph following the implantation of the femur.

On the 3-month CT scan post-placement of the 3D-printed cage into the distal left femur, there is evidence of significant osseointegration, which measures 114 mm in circumferential dimension, compared to a small gap of 9 mm anteromedially in the bone (i.e. about 92.1 % osseointegration). Furthermore, the small persisting gap is only noted at the distal 2.2 cm of the area covered with the 3D-printed cage, out of a total length of 8.9 cm covered by the material, which represents 25 % of the total length. There has, therefore, been complete osseointegration over the proximal 75 % of the area of concern. In the present study, further assessment of osseointegration at the EPORE material bone interface using the Zone Score showed that the number of bone-EPORE material bone interface junctions where osseointegration is observed is scored 4 out of 4 (2 points on AP and 2 points on lateral film, as shown in Fig. 4A and B). Utilizing the on-growth grading system, osseointegration is noted in at least 3 zones on the plain films, therefore resulting in Grade 4, which is the highest grade described. In addition, a low attenuation bone marrow density was present within the

entire intramedullary cavity of the 3D printed implant. Supplementary Figs. 1A–H at 3-months and Supplementary Figs. 2A and B at 12-months show bone union and sufficient osseointegration of the EPORE.

One month post mobilization in our physiotherapy department he started to complain of pain in his left tibia. His tibia wound was inflamed with abnormally elevated levels of C-reactive protein (CRP), Erythrocyte Sedimentation Rate (ESR), white blood cell count (WBC), indicative of infection. X-rays revealed loosening of metalwork and loss of reduction on his left tibia. He developed an abscess and wound dehiscence. The tibial metalwork was removed with an extra 1-cm of necrotic bone, and an external fixator system was applied with a PMMA cement spacer in the bone gap. Microbiology cultures (tissue and removed implants sonication fluid) developed of Methicillin-resistance-*Staphylococcus aureus* sensitive to vancomycin. The patient received a 6-week course of IV Vancomycin. The bone cement spacer was removed at 6 weeks, through an incision in the PMMA-induced membrane, bone allograft, as well as iliac crest graft was put into the gap and the LRS was compressed 3-cm acutely as shown in Fig. 3B. IV Vancomycin was given for another 6 weeks. The patient was able to mobilize fully- weight bearing using a Zimmer frame. The tibial fracture united clinically and radiologically 12- months after the application of LRS and the insertion of bone graft within the Masquelet tibial induction membrane, as shown in Fig. 5A. During the12-month follow-up period the patient developed recurrent pin site infections, requiring oral, as well as intravenous antibiotics. The pin site related infections finally settled down, after the external fixator was removed, surgical debridement of the pin site tracks was performed and a final 6-week course of oral antibiotics was prescribed. CT scan images obtained during his final readmission for the tibial fracture revealed satisfactory progress of tibial union as well as stable internal fixation and osseointegration of the customized 3D-printed implant at the femur, as shown in Fig. 5B.

Our patient's informed consent was obtained that data concerning his case would be published.

Discussion

Open distal femur fractures constitute 5–10 % of all distal femoral fractures. They are contaminated; they occur mainly in poly-trauma patients and are complicated by extensive bone loss [12]. These fractures are at risk for infection, mal-union, post-traumatic arthritis and impaired function. Aggressive bone and soft tissue debridement is of paramount importance to reduce the potential infection risk. The large bone defects following surgical debridement, often require an increased number of operative procedures to achieve bone union.

Definitive internal fixation options include intra-medullary nails, locking plates, as well as their combinations (nail and plate or a combination of a laterally based and a medially based plate). Multiple comparison clinical studies of these implants in open femoral fractures, do not demonstrate significant differences in a variety of outcomes between nails and laterally based anatomic plates [12]. The combination of two plates or of plate and a nail seem to offer improved clinical outcomes in terms of union rates and reduced number of operations in comminuted distal femoral fractures. Comminuted distal femoral fractures without massive bone loss are the main reason that surgeons opt for double plating [13,14].

Bone loss is dealt with staged cortico-cancellous autograft and fibular strut grafting. However, healing is incomplete, when diaphyseal defects are longer than 6 cm, because of graft resorption even in a well-vascularized muscle envelope. Large gaps require, more than one site to harvest the graft, adding to patient morbidity [15]. Vascularized bone grafts fare much better, but are technically demanding and donor sites are limited. Allograft has its limitations (preparation and preservation) and its problems as well [15].

An increased risk of treatment failure has been reported for major defects exceeding 80 cc in volume [16]. Defects exceeding 8 cm in length are less likely to achieve union regardless of how the defect is managed [16].

The Ilizarov technique for major bone loss requires a great deal of expertise to perform successfully. The treatment process is slow and can be painful. To prevent permanent joint stiffness, extreme patient compliance and prolonged physiotherapy are required. Up to 8 % non- union rates and 12.5 % poor functional results has been reported in open distal femoral fractures [17]. Complications during bone transport, include failure of the bone segment to join to the docking site (non-union), pin tract infection, loosening, or breakage, delayed consolidation of the bone, and cellulitis [18].

MIMT was developed in 1986 to address defects larger than 15 cm. It relies on the development of a bioactive foreign body-induced membrane that consolidates massive cancellous bone grafts. This membrane is full of growth factors reaching their highest level at the fourth week [19]. Some patients treated with MIMT suffer from acute trauma but most patients (90 %) have established non-unions. These patients have an average of 2–3 previous surgeries. Almost half of them present with active infections [20].

MIMT has been used with standard osteo-synthesis implants in acute distal femoral fractures with major bone loss. It seems that immediate unrestricted weight bearing and aggressive postoperative physiotherapy was not always possible in these cases. Knee stiffness has been reported; despite a successful union at an average of only 4 months following the second stage operation, when the bone graft was inserted and a medial plate was applied [12].

Lindsey et al. [21] and Attias et al. [22], were the first to report the use of a Cylindrical Titanium Mesh Cage just to contain cancellous bone graft and treat large segmental bone losses. O'Malley and Kates [23] first described the hybrid MIMT, where a titanium cage was used during a 2-stage reconstruction into an induced foreign body membrane.

The mechanical and structural stability of load-sharing 3D implants offer the advantage of immediate full weight bearing in cases of massive juxta-articular distal femoral bone loss, when other techniques are considered unsuitable.

In a case series of segmental distal femoral bone defects, patient-specific, 3D printed titanium cages were used successfully in 5 patients (male 3, female 2) to reconstruct femoral defects in 3 fractures and 2 infected non unions with a 2-stage hybrid MIMT.

The mean reconstructed femoral defect measured 14.0 cm (10.3–18.4) in length. The mean bone defect volume was 192.4 cc (114–292 cc). The authors however did not report the length of time it took the cage to incorporate into the host bone [24].

Another study explored the clinical outcomes in 9 cases who were treated with customized 3D- printed porous tantalum scaffolds

Table 1
Direct intra-operative costs.

Parameters	Combined (femur and tibia)	Femur	Tibia
	1st surgery Cross knee external fixation	2nd surgery ORIF and 1st stage Hybrid MIMT-PMMA cement×2 3rd surgery Hybrid (titanium cage and bone graft) Masquelet induction membrane technique (MIMT) and bone graft	3rd surgery ORIF×2-DCP locking plates and bone graft 4th surgery Removal of metalwork, LRS external fixation and 1st stage conventional MIMT (PMMA cement ×1) 5th surgery 2nd stage conventional MIMT (bone grafting) and compression 6th surgery Removal of LRS and HA coated pins
Intra-operative direct costs	Hoffman II Ex-Fix: € 2900 Blood transfusion×4: € 1200 (1st surgery). Blood transfusion ×2: € 600 (2nd surgery). Blood transfusion ×2: €600 (3rd surgery). Antibiotics 1st, 2nd and 3rd surgery: €90	EPORE-Implant: €11,000 Plating of femur (AXSOS): €834.68 Cements ×2: €100 Pulse-lavage: €120 Bone graft 80 cc (RIA autograft and allograft human): €3427.69	LRS tibia: €2950 Hydroxyapatite coated pins: €306 ORIF tibia: €1900 Cement ×1: €50 Blood transfusion ×2 units: €600 Antibiotics: 4th, 5th and 6th surgery: €125 Bone graft 50 cc (RIA autograft and allograft human): €2142.3
Total amount	€4190	€15,482 (€1720/cm of bone gap)	€8074 (€2691/cm of bone gap)

Abbreviations: ORIF: open reduction and internal fixation, PMMA: poly-methyl-methacrylate; DCP: dynamic compression plate; LRS: limb reconstruction system (Orthofix); RIA: reamer irrigator aspirator.

combined with Masquelet's induced membrane technique to reconstruct infective segmental femoral defects (length:10.2–19.8 cm) was reported by Wu Y et al. [3]. All patients achieved sufficient deformity correction as well as length of limb and postoperative radiological exams revealed stable internal fixation and osseo-integration [3].

A limitation with our case report is the different bone and differing indications for Masquelet (infection in the case of the tibia), in which the techniques were employed.

However according to Masquelet [6,7], the technique's effectiveness and efficiency are proven irrespective of the bone it has been used so far. Meticulous debridement of nonviable bone at both stages of the technique, is of paramount importance for a successful outcome. Provided that all non-viable and infected tissue is removed, bone healing of the osseous defect is independent of its size [7].

A recent case series where Masquelet technique has been applied across different bones and different bone regions, has shown the technique to be versatile and effective in addressing diaphyseal, metaphyseal, epiphyseal bone defects in different bones, when massive bone loss is an issue [24].

Another limitation is the possibility of infection of such a large implant. Orthopaedic implant use increases infection risk in general. The infection risk can be explained by the "race for the surface" concept, where there is competition between host-cell integration and bacterial colonization [25]. When the host cells colonize rapidly the implant's surface, the probability of bacterial colonization is very low [25].

EPORE® utilizes tiny rods of Titanium (~ 350 μm) which are arranged together in an open stochastic random pattern to form 'pores' of 100–500 μm, similar to that of trabecular bone. It has osteoconductive as well as osteoinductive properties [26].

At 3-months following the insertion of the EPORE 3-D printed custom –made implant, our radiologists reported bone growth on all surfaces of the implant, union at the interfaces between bone and implant, and bone growth in the cylindrical cavity of the implant, that was in continuity with the femoral intra-medullar cavity.

We hypothesize that bone in-growth on the implant's surface was rapid for three main reasons:

a) the induction membrane has spontaneous osteogenic activity [27,28] and an immune barrier capacity preventing microbial colonization [3]. The induction membrane consists of a collagenous matrix containing a combination of mature vessels, microvessels, and capillaries densely distributed throughout the tissue, allowing antibiotics to penetrate into newly formed bone tissue. Macrophages are present throughout all induced membranes, especially in areas of high cell and vascular density as well as in a very distinct zone immediately adjacent to the PMMA spacer [3].
b) the patient's traumatic brain injury [9] and
c) the use of EPORE Titanium [26].

It has been of great interest to notice that standard ORIF of the patient's closed left proximal tibia was infected postoperatively. In contrast the 9 cm custom-made implant, which was inserted into a Masquelet Induction Membrane to treat an open femoral fracture, did remain immune to infection.

Our case is the first to report that insertion of a 3D-printed load-sharing construct loaded with bone graft, into a Masquelet Bioactive Induced Membrane has been advantageous, compared to the original Masquelet technique. Following insertion of the femoral custom-made implant, the femur had been clinically sound, allowing immediate full weight bearing. It is now over three years following insertion of the 3D-printed cage and the patient has been confident to fully weight bear on his left femur throughout the whole follow

Table 2
Operative theatre time: 6 (six) times our patient was taken to theatre for surgery related to his left femoral and tibia fractures.

Combined surgery × 3 (femur and tibia)	Combined (femur and tibia) operative theatre time = 14 h and 25 min (60 % femur-40 % tibia)
Surgery × 3 exclusively on his left tibia	Tibia operative theatre time = 11 h and 5 min

Table 3
Outpatients costs.

Outpatient costs related to tibia	Outpatient costs related to femur
Outpatients' attendance: 6 follow up visits (€50 per attendance) during 13 months: €300	Outpatients' attendance: 2 follow up visits (€50 per attendance) during 13 months: €100
Outpatients' imaging: 8 set of x-rays Ap/lat and 2 CAT scans: €460	Outpatients imaging: 2 set of x-rays Ap/lat and 1 CAT scan: €260
Outpatients' physiotherapy (1 NHS OPD physiotherapy €25) × 20 = €500	Ambulance transport (€40-each×2) = €80
Ambulance transport (€40-each×18) = €720	
Outpatients' IV and oral antibiotics for tibia = €250	
Outpatients' hematology and biochemistry tests = €90	
Total amount: €2320	Total amount: €420

up period. During his last out- patient appointment the patient stated he "had forgotten surgery on the thigh" following his suture removal. At three months following implantation of the 3D printed implant in the femur, we were able to see early surface bone in-growth as well as incorporation at the host– implant junction proximally and distally. In the tibia despite a significantly smaller defect, the CT scan revealed union 12 months after the second stage of MIMT. Compared to all other traditional methods of external or internal fixation we could have used in conjunction with MIMT, the 3D-printed load-sharing cage, did allow immediate post operative, constant as well as reliable full weight-bearing ability throughout the follow-up period.

The sum of all direct costs paid on behalf of the patient by the Hellenic National Insurance (HEOPPY) has been €49,678 (inpatient as well as outpatient costs). We did collect data to evaluate direct intra-operative and outpatient costs (Tables 1, 2, 3), according to a pilot study comparing direct costs on tibial bone defects, between fine wire circular fixator (ILF) and the Masquelet technique using internal fixation (MIF) [29]. However, we were not able to obtain data about the intra-operative cost of theatre time in our hospital. Considering the above limitation our overall direct intra-operative costs were higher (€15,482) in the femur compared to the tibia (€8074), due to the use of an expensive (€11,000) 3D-printed load sharing cage. The direct intra-operative cost per cm of bone gap treated [29] was €2691/cm in the tibia, whilst the direct intra-operative cost for the femur in our case has been €1720/cm bone gap (Table 1), excluding the cost of the drill bits, the cost of sterilization of kits, k-wires, as well as the theatre cost from the first combined surgery (cross knee external fixation). In case we performed an original Masquelet technique in the femur with an additional medial ORIF and used an extra 30 cc of bone graft instead of the EPORE implant, the estimated direct operative cost to treat our femoral bone gap, would have been €6582 (€732/cm of bone gap).

Kanakaris's et al. reported £3944/cm of tibia bone gap, when cost of theatre time is included [29]. We note that in Kanakaris's paper, direct only intra-operative costs were £2093/cm bone defect treated (including theatre time and other costs that we did not include in our calculation such as cost of drill bits, cost of sterilization, k-wires etc.). Kanakaris et al. included all related theatre costs into their analyses. We excluded the combined (femur and tibia) cost of1stSurgery (€4190-Table 1), whilst calculating the direct operative cost/cm of bone gap for the femur and tibia separately.

The total amount of theatre time required to deal with the left tibia fracture was twice as much compared to the total amount of time needed to deal with the femoral fracture (Table 2). The out-patients' direct costs were higher for the tibia fracture as well (Table 3).

Most financial losses for fracture patients however are not due to direct costs of medical treatment, but from indirect costs due to loss of working wages. It has been reported that financial indirect costs increase up to CD $458 per each week of delay for the definitive treatment of a lower limb fracture [30]. As our patient was a right trans-femoral amputee with a capacity to fully weight bear without pain on his left distal femur, almost immediately postoperatively, we did consider that increased direct intra-operative cost was probably justified in this particular case.

In conclusion, in relation to his large 9 cm osseous femoral defect, we think that our patient received a successful treatment. However systematic prospective studies are needed to assess the direct medical, direct non- medical, indirect, and monetized quality of life (QALY-quality adjusted life/year), before any innovative surgical intervention enters into general clinical use [31,32].

Supplementary data to this article can be found online at https://doi.org/10.1016/j.tcr.2024.100978.

CRediT authorship contribution statement

Athanasios F. Foukas: Writing – review & editing, Writing – original draft, Visualization, Methodology, Investigation, Formal analysis, Conceptualization. **Argyris C. Hadjimichael:** Writing – review & editing, Writing – original draft, Visualization, Software, Resources, Investigation. **Christophoros Nicolaou:** Validation, Methodology. **Olga D. Savvidou:** Visualization, Validation, Supervision. **Panayiotis J. Papagelopoulos:** Visualization, Validation, Supervision.

Declaration of competing interest

The authors declare that they have no known competing financial interests or personal relationships that could have appeared to influence the work reported in this paper.

Acknowledgement

This study was supported financially by Implant cast Hellas. The sponsor manufactured the 3D-printed load sharing implant and funded the submission fees of the published article. Implant cast Hellas was not involved in the collection, analysis, and interpretation of data or in the writing of the report and the decision to submit the article for publication.

References

[1] R.J. Kadakia, C.M. Wixted, N.B. Allen, A.E. Hanselman, S.B. Adams, Clinical applicationsof custom 3D printed implants in complex lower extremity reconstruction, 3D Print Med. 6 (1) (Oct 2 2020) 29, https://doi.org/10.1186/s41205-020-000834 (PMID:33006702; PMCID:PMC7531160).
[2] Ballard DH, Mills P, Duszak R Jr, Weisman JA, Rybicki FJ, Woodard PK. Medical 3D printing cost-savings in orthopedic and maxillofacial surgery: cost analysis of operating room time saved with 3D printed anatomic models and surgical guides.Acad. Radiol.2020Aug;27(8):11031113.doi:https://doi.org/10.1016/j.acra.2019.08.011.Epub2019Se p18. (PMID: 31542197; PMCID: PMC7078060).
[3] K. Tetsworth, A. Woloszyk, GlattV.3D printed titanium cages combined with the Masquelet technique for the reconstruction of segmental femoral defects: preliminary clinical results and molecular analysis of the biological activity of human-induced membranes, OTA Int. 2 (1) (Mar 12 2019) e016, https://doi.org/10.1097/OI9.0000000000000016 (PMID:33937652; PMC7953522).
[4] Y. Wu, X. Shi, S. Zi, M. Li, S. Chen, C. Zhang, Y. Xu, The clinical application of customized3D-printed porous tantalum scaffolds combined with Masquelet's induced membrane technique to reconstruct infective segmental femoral defect, J. Orthop. Surg. Res. 17 (1) (Nov 5 2022) 479, https://doi.org/10.1186/s13018-022-03371 (PMID:36335402; PMCID:PMC9636627).
[5] MizobataY., Damage control resuscitation: a practical approach for severely hemorrhagic patients and its effects on trauma surgery, J. Intensive Care 5 (1) (Jan 20 2017) 4, https://doi.org/10.1186/s40560-016-0197-5 (PMID: 34798697; PMCID: PMC8600903).
[6] A.C. Masquelet, J. Sales de Gauzy, T. Bauer, A. Fabre, F. Fitoussi, D. Hannouche, et al., Reconstruction des pertes de substance osseus ediaphysair esd'originetraumatique, Strategies, recommandations, perspectives. Rev Chir Orthop Traumatol. 98 (1) (2012) 94–103.
[7] Masquelet A, Kanakaris NK, Obert L, Stafford P, Giannoudis PV. Bone repair using the Masquelet technique. J. Bone Joint Surg. Am. 2019Jun5;101(11):1024–1036.doi:https://doi.org/10.2106/JBJS.18.00842.(PMID: 31169581).
[8] Y. Lu, J. Wang, Y. Yang, Q. Yin, Bone defects are repaired by enhanced osteogenic activity of the induced membrane: a case report and literature review, BMC MusculoskeletDisord. 22 (1) (May 15 2021) 447, https://doi.org/10.1186/s12891-021-04317-2 (PMID: 33992104; PMCID: PMC8126171).
[9] A.J. Hotchen, L.V. Barr, M. Krkovic, Bridging hard callus at 48 days in an open femoral shaft fracture with segmental defect treated with a first-stage Masquelet technique: I wasn't expecting that, Strategies Trauma Limb Reconstr. 13 (1) (Apr 2018) 57–60, https://doi.org/10.1007/s11751-017-0300-z (Epub 2017 Nov 7. PMID: 29116576; PMCID: PMC5862707).
[10] B. Davies, R. Kaila, L. Andritsos, C. Gray Stephens, G.W. Blunn, C. Gerrand, P. Gikas, A. Johnston, Osteointegration of hydroxyapatite-coated collars in cemented massive endoprostheses following revision surgery, Bone Jt Open. 2 (6) (Jun 2021) 371–379, https://doi.org/10.1302/2633-1462.26.BJO-2021-0017.R1 (PMID: 34134510; PMCID: PMC8244796).
[11] T. Haider, I. Pagkalos, G. Morris, M.C. Parry, L.M. Jeys, Early radiographic osseointegration of a novel highly porous 3D-printed titanium collar for megaprostheses compared to a previous generation smooth HA-coated collar, Arch. Orthop. Trauma Surg. 143 (8) (Aug 2023) 4671–4677, https://doi.org/10.1007/s00402-022-04760-3 (Epub 2023 Jan 4. PMID: 36598605; PMCID: PMC10374805).
[12] T.R. Dugan, M.G. Hubert, P.A. Siska, H.C. Pape, I.S. Tarkin, Open supracondylar femurfractures with bone loss in the polytraumatized patient - timing is everything!, Injury 44 (12) (Dec 2013) 182631, https://doi.org/10.1016/j.injury.2013.03.018 (Epub 2013 Apr 16 .PMID:2 3601115).
[13] M.G. Bologna, M.G. Claudio, K.J. Shields, C. Katz, T. Salopek, E.R. Westrick, Dual plate fixation results in improved union rates in comminuted distal femur fractures compared to single plate fixation, J. Orthop. 18 (Sep 15 2019) 76–79, https://doi.org/10.1016/j.jor.2019.09.022 (PMID: 32189888; PMCID: PMC7068022).
[14] K. Stoffel, C. Sommer, M. Lee, T.Y. Zhu, K. Schwieger, C. Finkemeier, Double fixation for complex distal femoral fractures, EFORT Open Rev. 7 (4) (Apr 21 2022) 274–286, https://doi.org/10.1530/EOR-21-0113. PMID: 35446259; PMCID: PMC9069857.
[15] Hertel R, Gerber A, Schlegel U, Cordey J, Rüegsegger P, Rahn BA. Cancellous bone graft for skeletal reconstruction. Muscular versus periosteal bed—preliminary report. Injury 1994;25 Suppl 1:A59–70. doi:https://doi.org/10.1016/0020-1383(94)90263-1. (PMID: 7927661).
[16] J. Muhlhausser, J. Winkler, R. Babst, et al., Infected tibia defect fractures treated with the Masquelet technique, Medicine(Baltimore). 96 (2017) e6948.
[17] R. Kumar, S.S. Mohapatra, N. Joshi, S.K. Goyal, K. Kumar, R. Gora, Primary Ilizarov external fixation in open grade III type C distal femur fractures: our experience, J Clin Orthop Trauma 10 (5) (Sep-Oct 2019) 928–933, https://doi.org/10.1016/j.jcot.2019.01.026 (Epub2019Jan 30. PMID: 31528070; PMCID: PMC6738496).
[18] Abdel-Aal AM. Ilizarov bone transport for massive tibial bone defects. Orthopedics 2006Jan;29(1):70–4. doi:https://doi.org/10.3928/01477447-20060101-10. (PMID:16429937).
[19] T.F. Raven, A. Moghaddam, C. Ermisch, F. Westhauser, R. Heller, T. Bruckner, G. Schmidmaier, Use of Masquelet technique in treatment of septic and atrophic fracture non-union, Injury 50 (Suppl. 3) (Aug 2019) 40–54, https://doi.org/10.1016/j.injury.2019.06.018 (Epub2019 Aug1. PMID: 31378541).
[20] I. Morelli, L. Drago, D.A. George, E. Gallazzi, S. Scarponi, C.L. Romanò, Masquelet technique: myth or reality? A systematic review and meta-analysis, Injury 47 (Suppl. 6) (Dec 2016) S68–S76, https://doi.org/10.1016/S0020-1383(16)30842-7 (PMID: 28040090).
[21] Lindsey RW and Gugala Z. Cylindrical titanium mesh cage for the reconstruction of long bone defects. Osteosynthesis and Trauma Care 2004; 12(3): 108-115DOI:https://doi.org/10.1055/s-2004-822777.
[22] N. Attias, R.W. Lindsey, Case reports: management of large segmental tibial defects using a cylindrical mesh cage, Clin. Orthop. Relat. Res. 450 (Sep 2006) 259–266, https://doi.org/10.1097/01.blo.0000223982.29208.a4 (PMID: 16702918).
[23] N.T. O'Malley, S.L. Kates, Advances on the Masquelet technique using a cage and nail construct, Arch. Orthop. Trauma Surg. 132 (2) (2012 Feb) 245–248, https://doi.org/10.1007/s00402-011-1417-z (Epub 2011 Nov 11. PMID: 22072192).
[24] W.R. Daniel Seng, A.X. Rex Premchand, Application of Masquelet technique across bone regions - a case series, Trauma Case Rep. 37 (Dec 24 2021) 100591, https://doi.org/10.1016/j.tcr.2021.100591 (PMID: 35005167; PMCID: PMC8718970).
[25] A.G. Gristina, Biomaterial-centered infection: microbial adhesion versus tissue integration, Science 237 (4822) (Sep 25 1987) 1588–1595, https://doi.org/10.1126/science.3629258 (PMID: 3629258).
[26] A.M. Barradas, H. Yuan, C.A. van Blitterswijk, P. Habibovic, Osteoinductive biomaterials: current knowledge of properties, experimental models and biological mechanisms, Eur Cell Mater. 21 (May 15 2011) 407–429, https://doi.org/10.22203/ecm.v021a31 (discussion 429, PMID: 21604242).
[27] O.M. Aho, P. Lehenkari, J. Ristiniemi, S. Lehtonen, J. Risteli, H.V. Leskelä, The mechanism of action of induced membranes in bone repair, J. Bone Joint Surg. Am. 95 (7) (Apr 3 2013) 597–604, https://doi.org/10.2106/JBJS.L.00310 (PMID: 23553294).

[28] Q. Yin, X. Chen, B. Dai, J. Liu, Y. Yang, S. Song, Y. Ding, Varying degrees of spontaneous osteogenesis of Masquelet's induced membrane: experimental and clinical observations, BMC Musculoskelet. Disord. 24 (1) (May 15 2023) 384, https://doi.org/10.1186/s12891-023-06498-4 (Erratum in: BMC Musculoskelet Disord. 2023 Jul 27;24(1):616. PMID: 37189083; PMCID: PMC10184391).

[29] N.K. Kanakaris, P.J. Harwood, R. Mujica-Mota, G. Mohrir, G. Chloros, P.V. Giannoudis, Treatment of tibial bone defects: pilot analysis of direct medical costs between distraction osteogenesis with an Ilizarov frame and the Masquelet technique, Eur. J. Trauma Emerg. Surg. 49 (2) (Apr 2023) 951–964, https://doi.org/10.1007/s00068-022-02162-z (Epub 2022 Nov 28. PMID:36443494; PMCID: PMC10175460).

[30] S. Sprague, M. Bhandari, An economic evaluation of early versus delayed operative treatment in patients with closed tibial shaft fractures, Arch. Orthop. Trauma Surg. 122 (6) (Jul 2002) 315–323, https://doi.org/10.1007/s00402-001-0358-3 (Epub 2001 Dec 12. PMID: 12136294).

[31] Kanakaris NK, Giannoudis PV. The health economics of the treatment of long-bone non- unions. Injury. 2007 May;38 Suppl 2:S77–84. doi:https://doi.org/10.1016/s0020-1383(07)80012-x. Erratum in: Injury 2007 Oct;38(10):1224. (PMID: 17920421).

[32] B.U. Nwachukwu, W.W. Schairer, E. O'Dea, F. McCormick, J.M. Lane, The quality of cost- utility analyses in orthopedic trauma, Orthopedics 38 (8) (Aug 2015) e673–e680, https://doi.org/10.3928/01477447-20150804-53 (PMID:26270752).